Journal of ASTM International, Vol. 6, No. 10
Paper ID JAI102298
Available online at www.astm.org

Jared D. Hooser,[1] *Mingjun Wei,*[2] *Barry E. Newton,*[3] *and Gwenael J. A. Chiffoleau*[4]

An Approach to Understanding Flow Friction Ignition: A Computational Fluid Dynamics (CFD) Study on Temperature Development of High-Pressure Oxygen Flow Inside Micron-Scale Seal Cracks

ABSTRACT: Flow friction ignition of non-metallic materials in oxygen is a poorly understood heat-generating mechanism thought to be caused by oxygen flow past a non-metallic sealing surface. Micron-scale fatigue cracks or channels were observed on non-metallic sealing surfaces of oxygen components and could provide a leak path for the high-pressure oxygen to flow across the seal. Literature in the field of micro-fluidics research has noted that viscous dissipation, a heat-generating mechanism, may not be negligible as the flow dimension of the channel is reduced to the micron-scale. Results of a computational fluid dynamics study are presented and used to determine if temperatures developed in high-pressure driven micro-channel oxygen flows are capable of reaching the reported autogenous ignition temperature of non-metallic materials in oxygen.

KEYWORDS: flow friction ignition, viscous heating, oxygen fires, microchannel flow, cylinder valves, CGA 870 seals, computational fluid dynamics, stagnation heating

Introduction

Flow friction ignition is a theorized heat-generating mechanism that has been attributed to the cause of fires in oxygen systems. Flow friction ignition is believed to occur when oxygen gas flows across or impinges upon non-metallic materials. It may encompass a variety of gas dynamics such as stagnation heating and vortex flow [1]. Several other potential heat-generating phenomena have been proposed to help understand flow friction ignition, but it remains a poorly understood ignition mechanism. Torsion cold working of polymers, vortex tube effects, and polymer friction were investigated by Gallus and Stoltzfus with promising results, but flow friction ignition has yet to be recreated experimentally [2]. In this paper, flow friction ignition is studied in high-pressure micro-channels as a possible mechanism to ignite non-metallic seals in oxygen. A proposed micro-channel gas flow scenario is demonstrated and used as the basis to study frictional heating of high-pressure oxygen gas flow through micron-sized cracks in non-metallic seals. Computational fluid dynamics (CFD) is utilized to determine whether a critical crack configuration is capable of developing autogenous ignition temperatures (AITs) of select non-metallic materials in oxygen. This paper presents examples of fires attributed to flow friction ignition, micro-channel flow theory, a corresponding CFD model, and results of initial CFD simulations. The work is part of an ongoing research program and this paper represents the first stage of the program.

Background

Flow friction ignition has been attributed to the cause of oxygen fires shown to originate at non-metallic seals where no other known heat-generating mechanisms were believed to be present. Common ignition mechanisms such as adiabatic compression, particle impact, and promoted ignition are active only during rapid transients. When an ignition of a non-metallic material occurs, well after the end of rapid transients,

Manuscript received December 29, 2008; accepted for publication August 18, 2009; published online September 2009.
[1] MSME, Wendell Hull and Associates, Inc., 5605 Dona Ana Rd., Las Cruces, NM 88007.
[2] Assistant Professor, Dept. of Mechanical and Aerospace Engineering, New Mexico State Univ., Las Cruces, NM 88003.
[3] VP R&D, Wendell Hull and Associates, Inc., 5605 Dona Ana Rd., Las Cruces, NM 88007.
[4] Senior Scientist, Test Facility Manager, Wendell Hull & Associates, Inc., 5605 Dona Ana Rd., Las Cruces, NM 88007.

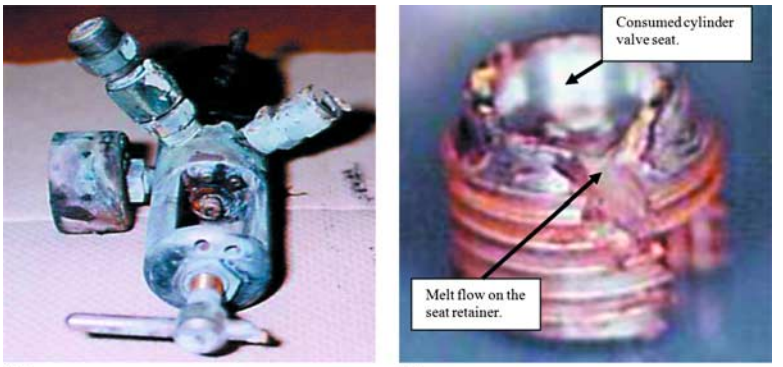

FIG. 1—*(a) Fire-damaged regulator; (b) the cylinder valve seat retainer showing consumption of the seat with melt flow erosion of the seat retainer.*

flow friction ignition is often attributed to the cause of the fire because of the lack of other credible ignition mechanisms.

The following examples are a selection of medical oxygen fires investigated by Wendell Hull Associates, Inc. (WHA) and other reported fires believed to be caused by flow friction ignition. In these fires, non-metallic seals were the probable points of origin and warrant the possibility of flow friction ignition.

WHA Medical Oxygen Flow Friction Ignition Fires

Oak Creek, Wisconsin Fire Department Fire—An oxygen fire occurred in 1999, when a firefighter opened a cylinder valve connected to a medical oxygen regulator being used on an emergency medical service vehicle. The individual indicated that the fire occurred immediately after opening the cylinder valve. There was a sudden eruption of flame from the regulator. An investigation into the fire's origin concluded that initial ignition occurred at the cylinder valve's non-metallic seat, which caused the fire to propagate from inside the cylinder valve to the internal components of the regulator, resulting in fire damage to the regulator's aluminum body. The fire-damaged regulator and seat retainer are shown in Fig. 1. The cylinder valve seat was identified as polyphenylene oxide (PPO), a plastic material known to deteriorate, extrude, and exhibit material loss during normal service. It was suspected that the PPO seat had degraded over time, which caused surface irregularities in the oxygen flow stream. That condition would have increased the exposure of the cylinder valve seat to the gas flow and increased the likelihood of generating localized heating of the seat.

Alleghany Regional Hospital Incident—Another oxygen fire occurred in 1999, when a patient was receiving medical oxygen at a hospital. The medical staff set a regulator to administer approximately 4 LPM of oxygen. The patient was reported to take one to two breaths before coughing and removing the nasal cannula. The investigation into the fire's origin concluded that the fire was focused inside the cylinder valve with the only fire damage resulting in near total consumption of the cylinder valve's non-metallic seat. The oxygen regulator assembly, which safely contained the fire event, and cylinder valve seat retainer are shown in Fig. 2. Burn residues on the cylinder valve seat retainer revealed the presence of a plastic seat similar to polychlorotrifluoroethylene (PCTFE). PCTFE seats have been used successfully in oxygen systems, but WHA and National Aeronautics and Space Administration (NASA) testing indicated some batches of the plastic were prone to substantial flow (mechanical instability) and tended to severely extrude within the seat retainer. Metal-to-metal wearing of the seat retainer was also consistent with extreme extrusion of the cylinder valve seat. Seat wear and extrusion would have increased leak paths and increased the opportunity for oxygen gas to generate heat as it flowed across the seal.

Howard County Maryland Fire Department Fire—A third oxygen fire occurred in 1999, at a fire station while conducting a leak test of a medical oxygen regulator. A popping sound was heard shortly after opening the cylinder valve and was followed by "fizzing" sounds. These audible sounds lasted for a few seconds prior to the regulator fire. An investigation into the fire's origin concluded that the fire originated at the CGA 870 sealing gaskets at the inlet to the regulator. The fire-damaged regulator and inlet

FIG. 2—*(a) Oxygen regulator assembly; (b) the cylinder valve seat retainer showing consumption of the cylinder valve seat.*

seals are shown in Fig. 3. A nylon crush gasket was found on top of an aluminum-bound rubber washer at the regulator inlet. Normally, only one gasket is used at the CGA 870 to seal the regulator and postvalve connection. Having two washers placed onto the regulator inlet does not allow proper insertion of the regulator onto the outlet of the cylinder valve. The improper installation of the sealing washers may have allowed oxygen to flow past the seals (i.e., external leak), thus increasing the likelihood of a flow friction ignition. The likelihood of adiabatic compression causing ignition of the seals was considered low due to the protection provided by the regulator inlet, although the gas heating from compression probably contributed to achieving the ignition temperature of the seal.

Additional Oxygen Fires Attributed to Flow Friction Ignition

Gallus and Stoltzfus reported on oxygen fires related to flow friction ignition [2]. One fire occurred in a dome loaded regulator at NASA White Sands Test Facility in 1986. A Viton diaphragm inside the regulator ignited and kindled the surrounding stainless steel body. Because the regulator was apparently static (i.e., no gas flowing) at the time of the incident, the fire's cause was attributed to flow friction ignition occurring at the Viton diaphragm (due to an external leak), which was consistent with the fire patterns. Oxygen fires also took place on commercial aircraft oxygen service carts. Investigators determined that Vespel seats within manual oxygen valves ignited and kindled the stainless steel valve stems, which caused fire to breech the brass valve housings. The cause of the fire was attributed to flow friction ignition initiated by weeping flow past the Vespel seats.

Observation of Micron-Scale Cracks on Nylon Oxygen Seals

Plastic materials are used to create gas seals over many cycles of use in oxygen systems. Over time, the continual loading of these seals against metal surfaces causes wear and surface irregularities to develop along the polymer surface. The following experiment identifies micron-scale surface cracks that can develop on the surface of a nylon valve seat through repeated use.

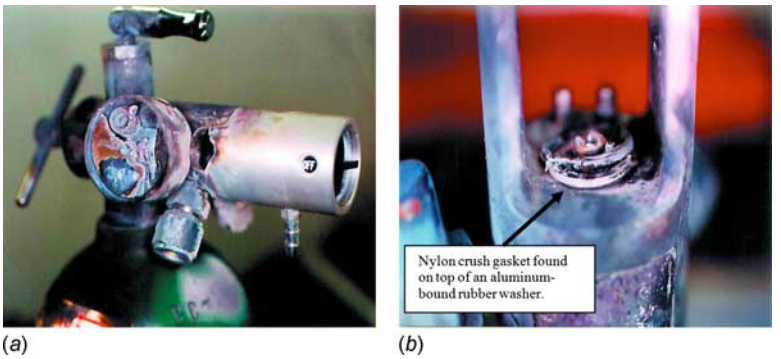

FIG. 3—*(a) Fire-damaged regulator; (b) inlet sealing.*

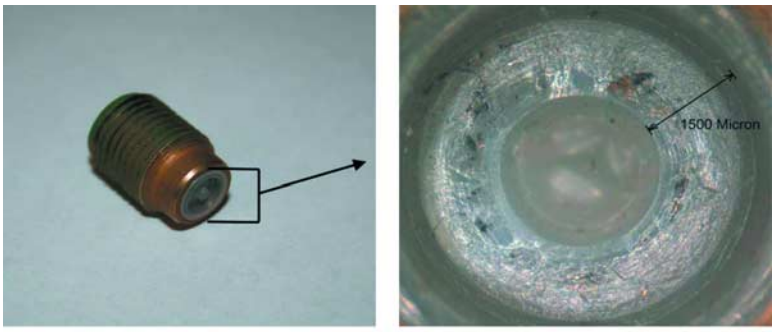

FIG. 4—*(a) Nylon seat removed from cylinder valve after the wear experiment; (b) 15× microscope enlarged view of the nylon sealing surface.*

An experiment was conducted on a nylon cylinder valve seat to demonstrate the development of surface micron-scale cracks, as shown in Fig. 4. A new oxygen cylinder valve was opened and closed approximately 100 times in order to expose the seat to a period of use and wear. Afterward, microscopic observation of the seal revealed the presence of micron-scale cracks extending radially across the surface of the seal (Fig. 5). Measurements of the cracks at various locations were obtained with a microscope to establish typical crack widths on the nylon surface. The measurements are tabulated in Table 1.

The presence of micron-scale cracks on the surface of polymer seals could allow high-pressure oxygen gas to flow across the sealing surface. This poses the question: Could oxygen flow confined to a micron-scale channel generate heat as it flows through these cracks? The presence of micron-scale cracks justified a CFD study that investigated the temperature development of oxygen gas flowing through micron-sized channels.

Viscous Dissipation in Micro-channel Flows

The flow of fluid through micron-scale devices has gained interest recently due to advances in micro-machining technology, which has allowed for practical development of micro-electromechanical systems and micro-fluidic devices. Micro-heat-exchangers that cool electronics, micro-pumps used to transport medicine to patients, and micro-heat-engines that generate electrical power are examples of these devices [3–5]. The need to predict the fluid behavior in micro-fluidic devices is highly desirable to properly validate designs pre-fabrication and has provided insight about the differences between micro-channel flows and large scale flows. Most of the research work involving temperature effects in micro-channel flows is related to heat transfer problems. Few research efforts have been directed at investigating viscous

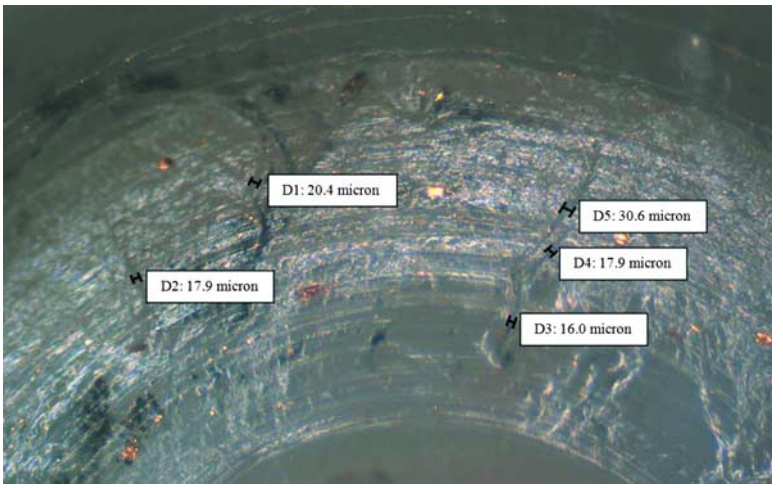

FIG. 5—*60× magnification of micron-scale cracking on the nylon cylinder valve seat shown in Fig. 4(b).*

TABLE 1—*Micron cracks measurements of nylon cylinder valve seat.*

Nylon Seal Crack Measurement	Crack Width (μm)
D1	20.4
D2	17.9
D3	16.0
D4	17.9
D5	30.6
Average width	20.6

dissipation effects and temperature development generated by a fluid flowing through micron-sized geometries.

Kundu and Cohen defined viscous dissipation as the rate of mechanical energy loss and a gain of internal energy through deformation of a fluid element [6]. The rate of viscous dissipation is proportional to the square of the velocity gradients and is important where fluids undergo high shearing stresses. The resulting heat generated by viscous dissipation can be intense; meteorites entering the Earth's atmosphere often burn up because of viscous dissipation heating that takes place between the air and meteor surface.

Researchers of viscous dissipation effects in micro-channels have suggested that the reduced flow dimension can increase the magnitude of viscous dissipation and frictional effects otherwise considered negligible in macro-scale flows. Koo and Kleinstreuer have analytically investigated the effect of diameter on viscous dissipation (i.e., temperature rise) in liquid micro-tubes and found that tubes less than 100 μm in diameter produced noticeable changes in fluid temperature, even for an isothermal wall condition [7]. The largest temperature rise reported was 25 K for a 20 μm diameter adiabatic tube with a Reynolds number of 2,000. Beskok and Karniadakis noted that the viscous heating terms for micro-domains may not be negligible [8]. They developed an analytical solution of a general micro-channel heat convection problem and showed an increase in the tangential temperature gradient along the surface of the pressure-driven channel as a function of increasing Mach number. The temperature profiles of their micro-channels with insulated surfaces produced the largest temperatures at the wall where shear stresses (i.e., viscous dissipation) dominated. To investigate frictional heating at the channel wall Wu et al. constructed a 20 $\times 2 \times 4,400$-micron channel with integrated temperature sensors [9]. Nitrogen gas at 1.87 and 2.10 MPa was forced through the thermally isolated channel. They reported that each temperature sensor reading was lower than the ambient gas temperature (297.87 K), but a sensor placed in between the inlet and outlet of the channel read the highest temperature (297.65 K). They attributed the highest temperature reading to frictional heating generated by the high-pressure gas flow.

Continuum Limit Considerations for Micro-channel Flow

Investigating pressure-driven oxygen flow through micron-scale cracks requires an understanding of fluid behavior when the characteristic dimension of the flow passage approaches the mean free path of the oxygen molecule. The mean free path describes the average distance traveled by a molecule before impacting another molecule. For oxygen, the mean free path is $2.98e^{-10}$ m which is only one order of magnitude different when compared to the length scale of the micron-scale cracks observed on the nylon seal in Fig. 5 (20 μm) [10]. For this reason, it was important to consider the limitations of continuum theory.

Continuum theory considers a continuous fluid and assumes all dependent variables like temperature, velocity, and density can be described as average quantities over a region that is large in comparison to the fluid particles but small in relation to the scale of the physical problem being described [11]. The Knudsen number (Kn) is used to distinguish continuum flows from free molecular flows (i.e., non-continuum flows). Table 2 outlines the difference between continuum and free molecular flows based on the Knudsen number.

The Knudsen number is defined as the ratio between the mean free path of the fluid molecule and the characteristic flow dimension

$$\mathrm{Kn} = \frac{\lambda}{L} \tag{1}$$

TABLE 2—*Knudsen number and corresponding flow regimes.*

Knudsen Number	Flow Regime
$Kn < 0.001$	Continuum
$0.001 < Kn < 10$	Slip/Transitional
$Kn > 10$	Free Molecular

$$\lambda = \frac{kT}{\sqrt{2}\pi p \sigma^2} \tag{2}$$

where:

λ = mean free path of the molecules,
L = characteristic length,
σ = molecular diameter,
k = Boltzman constant,
T = temperature, and
p = pressure [5].

Using Eq 2, a range of Knudsen numbers were calculated for different micro-crack widths for the expected temperature and pressure conditions at the inlet and outlet of the cracks[5] given in Table 3.

By varying the widths of the cracks from 1–200 μm and using the pressure and temperature values in Table 3, the Knudsen number was compared at the inlet and outlet of the cracks in Fig. 6(*a*). At the inlet, the Knudsen number was within the continuum limit for crack sizes larger than approximately 1 μm. At the outlet, the Knudsen number was greater than 0.001 for both temperatures, implying a non-continuum condition.

TABLE 3—*Expected values of pressure and temperature at the inlet and outlet of the micron-cracks.*

	Pressure, MPa	Temperature, K
Inlet	13.8	298–500
Outlet	0.1	298–500

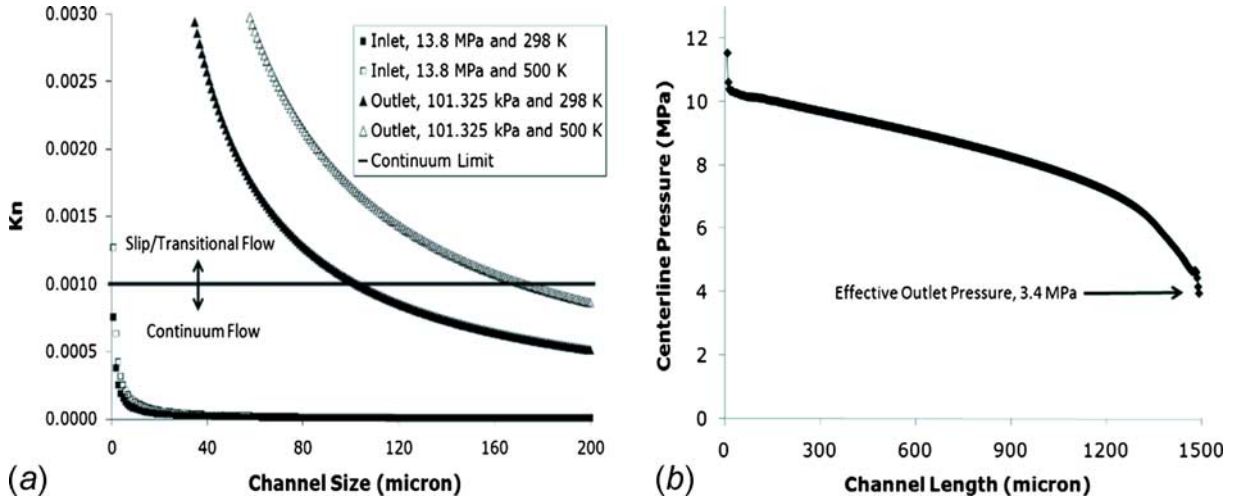

FIG. 6—*(a) Range of Knudsen numbers varying the channel width from 1–200 μm with inlet conditions of 13.7 MPa, and outlet conditions of 101.325 kPa at two temperatures; 298 and 500 K; (b) preliminary CFD centerline pressure distribution for a 20 μm width channel and the effective outlet pressure, 3.4 MPa.*

[5]Because oxygen tanks are typically filled with 13.8 MPa oxygen, this value was used as the inlet crack pressure. The pressure at the outlet of the crack was taken as atmospheric (0.1 MPa). The upper limit of temperature was chosen as 500 K because this is the nominal AIT of nylon in oxygen.

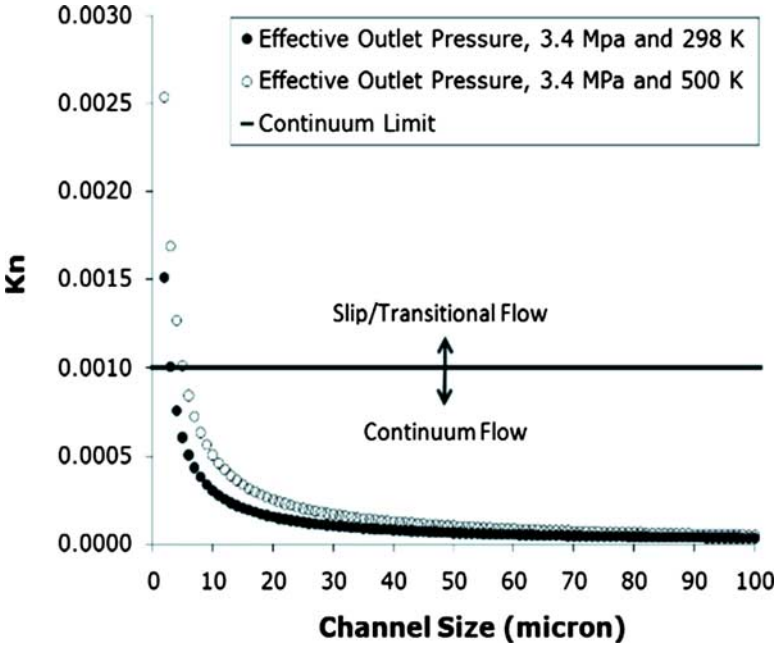

FIG. 7—*Range of Knudsen numbers at the channel effective outlet pressure, 3.4 MPa.*

However, preliminary CFD simulations indicated that the gas near the channel outlet maintained a higher pressure than the 0.1 MPa outlet boundary pressure. The centerline CFD pressure distribution for a 20 μm channel is shown in Fig. 6(*b*) highlighting the effective outlet pressure maintained near the channel outlet, approximately 3.4 MPa. Using the effective outlet pressure, the Knudsen number was within continuum limits at the outlet for crack sizes larger than approximately 8 μm (Fig. 7). Although gas expansion did not occur instantaneously at the outlet boundary, a major reduction in pressure existed after this point and the entire length of the micro-channel remained pressurized well above ambient pressure. Therefore, the gas flow up to the outlet boundary was expected to meet continuum conditions. Additional work is required to determine the crack size and channel pressure relationship with continuum flow.

Computational Fluid Dynamics Simulations with Fluent®

A steady two-dimensional turbulent compressible gas flow in a micro-channel was simulated using the CFD software, Fluent®. Temperature development in the micro-channels was investigated by varying the channel width, W, from 10–300 μm and length, L, from 500–10,000 μm. A schematic of the channel geometry is shown in Fig. 8.

Pressure-driven flow, consistent with an oxygen tank source feeding the inlet of the channel and exiting to atmosphere, was used to define the inlet and outlet boundary conditions of the model. Pressure boundaries were specified as 13.8 MPa and 0.1 MPa for the inlet and outlet, respectively, and gas temperature boundaries were maintained at 298 K. Boundary conditions at the channel walls were non-slip and adiabatic, which did not allow for any heat transfer to or from the surroundings. Heat transfer would normally occur in real micro-channel flows, but the adiabatic wall condition was chosen to readily compare heat development within each micro-channel flow.

A typical straight micro-channel configuration mesh is shown in Fig. 9. The same geometry and meshing approach was used for an enlarged inlet and outlet channel configuration by adding an enlarged region connected to the inlet and outlet of the channel (controlled by the channel height, h, illustrated in Fig. 10). To reduce computational time, only one-half the channel was simulated utilizing a symmetric boundary at the channel centerline. This configuration allowed for modeling of the oxygen gas flow entering and exiting the channel and resembles a closer representation of the real micro-channel crack flow situation.

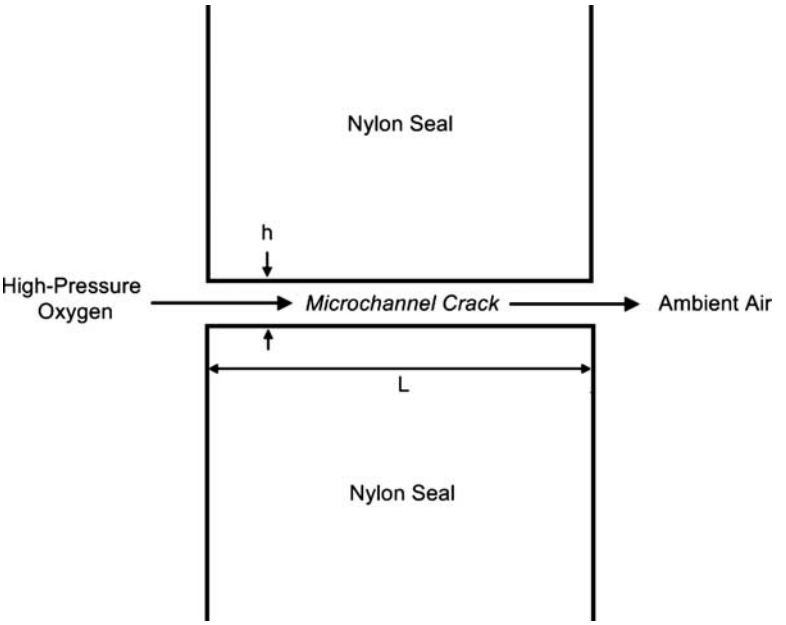

FIG. 8—*Two-dimensional micro-channel crack model for the Fluent® CFD study.*

Computational Fluid Dynamics Grid Independence Study

The simulation results depend on the size of the computational mesh chosen, especially at boundaries where large gradients are present in the flow field. To ensure the results obtained for the micro-channel simulations were independent of the computational mesh, it was necessary to perform several simulations with different mesh sizes for a single micro-channel geometry.

A 40 μm height by 1,500 μm length channel was chosen for the mesh independence study. A converged mesh was established when additional grid points added to the computational mesh produced less than a 0.2 % change in the simulation results. The computational mesh size was defined by grid points, which created grid intervals along a micro-channel edge. For example, if *N* grid intervals were desired

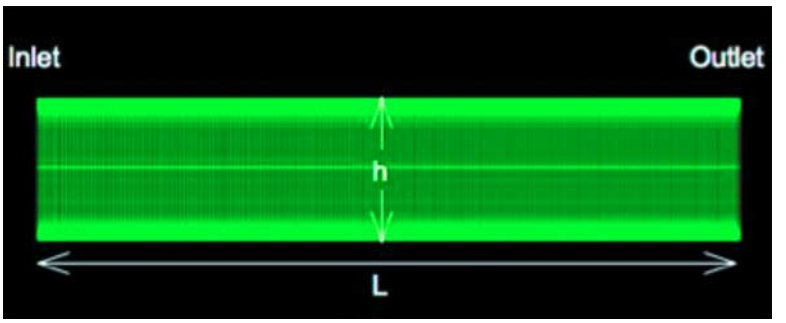

FIG. 9—*Typical straight micro-channel configuration mesh.*

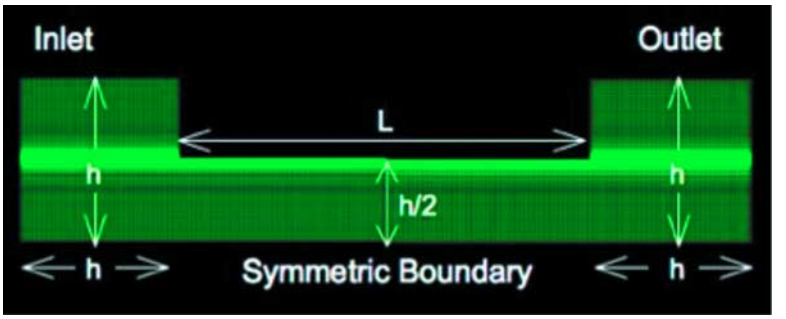

FIG. 10—*Micro-channel configuration mesh with an enlarged inlet and outlet region attached.*

TABLE 4—*Mesh refinements and corresponding velocity and temperature data.*

Refinement Level	Mesh Size	Midplane Velocity (m/s)	Midplane Wall Temperature (K)
1	10×250	246.247	286.828
2	20×250	252.472	290.117
3	40×250	248.142	291.456
4	40×500	247.857	291.461
5	60×500	247.460	292.315
6	60×750	247.384	292.314
7	80×500	247.551	292.914
8	80×750	247.470	292.915
9	90×500	247.926	292.985

along an edge, $N+1$ grid points are required along that edge. The computational mesh size was denoted by the number of grid intervals along the height and length directions (e.g., 50×100). Mesh independence was evaluated using velocity and temperature results obtained for each mesh refinement size at the channel midplane (a station located exactly between the channel inlet and outlet). The successive grid refinements and results for centerline velocity and temperature are given in Table 4. Refinement Level 7 was selected as the converged mesh because additional refinements (Levels 8 and 9) produced less than a 0.2 % change in the centerline velocity and wall temperature values.

Mesh Sizes for Different Channel Heights

To apply the converged mesh established for the 40 μm channel to channels of different heights, separate meshing techniques were used. This was dependent on whether the channel height was larger or smaller than the 40 μm height channel. If the channel height was less than 40 μm, the same mesh size established for the 40 μm channel mesh was used.[6] This was justified by assuming conservatively that the same amount of mesh cells within a smaller channel height dimension would achieve the same or better resolution demonstrated for the 40 μm converged mesh. If the channel height was larger than 40 μm, the boundary grid resolution was kept the same as the 40 μm converged mesh but additional grids were added to the center region of the channel to make up the increase in height. This approach limited the computational time required to perform mesh independence studies on all channel heights simulated. Table 5 shows the combination of micro-channel heights and lengths simulated with mesh sizes used.

Fluent® Simulation Results

The Fluent® simulation results are presented for both the straight and enlarged inlet and outlet attachment micro-channel configurations. Typical results for the effect of channel height and channel length on the midplane velocity and temperature profiles are given first followed by average wall and fluid temperatures compared against the dimensionless micro-channel aspect ratios, L/h, and Reynolds numbers, Re.

The effect of channel height and channel length on midplane velocity and temperature profiles are shown in Figs. 11–14. Small channel heights tend to reduce the magnitude of velocity and increase the magnitude of fluid temperature at the channel midplane. This result supports the increased influence of viscous forces generated by the micro-channel wall for smaller height channels; the closer the channel walls are to each other (small height distance) the more effect viscous forces will have across the small channel height. Conversely, channels with large heights (walls separated by a greater distance) were influenced less by viscous forces, as seen by the greater magnitude in midplane velocity and reduced midplane temperatures. The magnitude differences between midplane velocity and temperatures are noticeably different. Comparing the 10 μm and 300 μm height channels, centerline velocity and temperature values differed by 105 m/s and 26 K, respectively. A similar effect was seen when the channel length was varied with a constant channel height (Figs. 13 and 14). Long channel lengths tended to reduce the magnitude of the velocity and increase the magnitude of the fluid temperature at the channel midplane. This result corresponds to the additional friction force applied to the fluid flowing through a channel of

[6]Only 50 mesh cells were used for the 10 μm height channels because additional cells would result in a failed grid when imported into Fluent®.

TABLE 5—*Micro-channel simulation test matrix and mesh sizes used.*

	Channel Length (μm)				
Channel Height (μm)	500	1,500	3,000	5,000	10,000
10	50×167	50×500	50×1,000	50×1,667	
20	80×167	80×500	80×1,000	80×1,667	80×3,334
40	80×167	80×500	80×1,000	80×1,667	
60	94×167	94×500	94×1,000	94×1,667	
80	108×167	108×500	108×1,000	108×1,667	
100	122×167	122×500	122×1,000	122×1,667	
150	157×167	157×500	157×1,000	157×1,667	
200	192×167	192×500	192×1,000	192×1,667	
300	262×167	262×500	262×1,000	262×1,667	

longer length. Conversely, channels of shorter length have a reduced amount of frictional force applied along the wall and correspondingly have higher velocity and lower temperature magnitudes at the channel midplane. The differences in magnitude are again noticeably different. Comparing the 0.5 mm and 10 mm length channels, centerline velocity and temperature values taken from the midplane profiles differ by 126 m/s and 25 K, respectively.

The non-dimensional aspect ratio, L/h, and Reynolds number, Re, were chosen to identify fluid temperature trends throughout the range of micro-channel sizes simulated. The relationship between micro-channel aspect ratio and average wall and fluid temperatures is shown in Figs. 15 and 16. Micro-channels with short heights and long lengths (i.e., large aspect ratios) maintain higher average wall and fluid temperatures than channels with large heights and short lengths (i.e., small aspect ratios). This result corresponds to the previously presented channel midplane results in which channels with short heights and long lengths had larger temperature magnitudes than channels with large heights and short lengths. The relationship trend between aspect ratio and fluid temperature tends to flatten for aspect ratios larger than 100. This indicates an approach to an asymptotic limit, corresponding to approximately 290 K and 297 K for average fluid temperature and average wall temperatures, respectively. This result suggests that the upper limit of fluid temperature increase was approached with the micro-channel sizes simulated in this study. Also, channels with the same aspect ratio but different height/length combinations had comparable fluid temperatures. This indicated a strong correlation between channel aspect ratio and the temperature within the micro-channel flow field. The average fluid and wall temperatures were also compared against

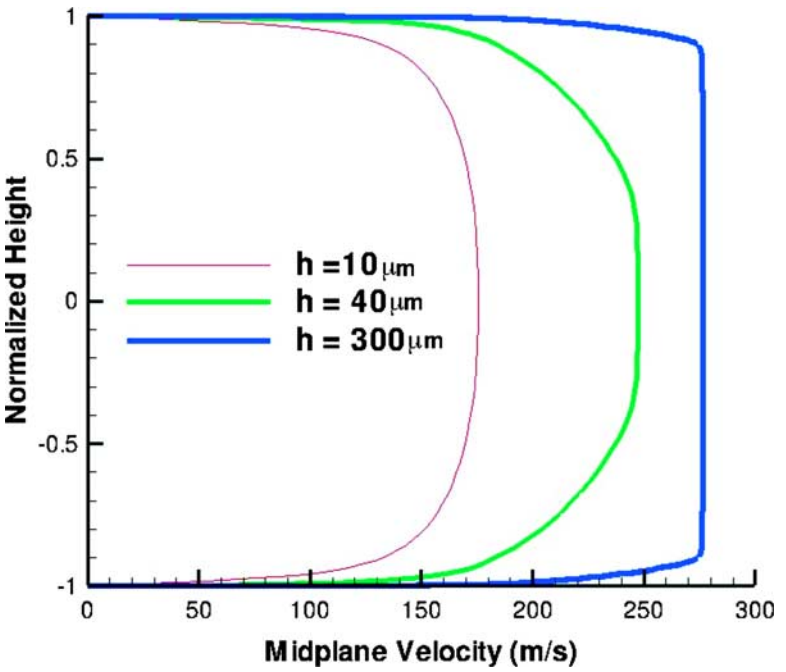

FIG. 11—*Micro-channel height effect on the midplane velocity profile.*

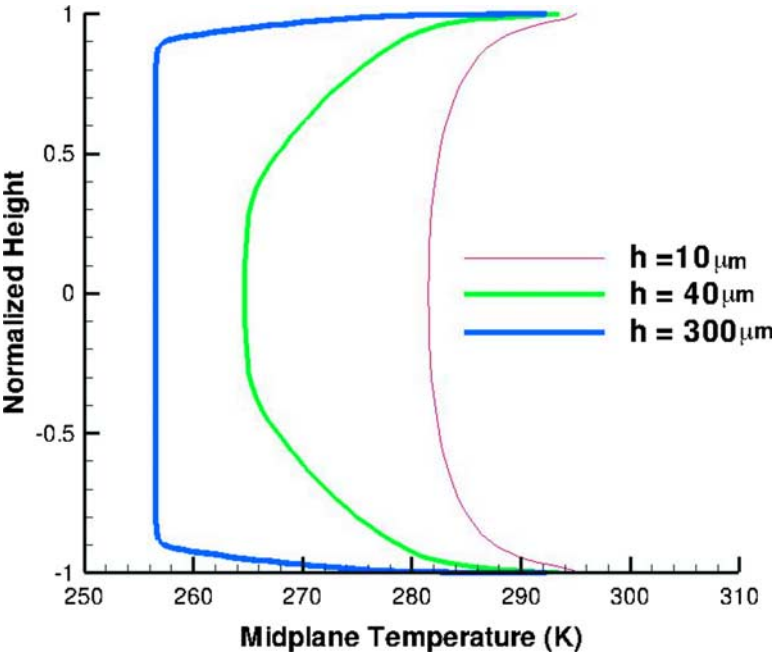

FIG. 12—*Micro-channel height effect on the midplane temperature profile.*

the channel Reynolds numbers in Figs. 17 and 18. As the Reynolds number decreases, average fluid and wall temperatures tend to increase, corresponding to a reduction in channel height and an increase in channel length. Because the Reynolds number is a ratio of the inertial and viscous forces in a flowing fluid, this result suggested that the inertial forces diminished with decreasing channel height and increasing channel length, thus allowing viscous effects to become more prominent (i.e., higher average fluid and wall temperatures due to friction at the channel wall).

An unusual trend was observed for the average wall temperature results obtained for channels with the inlet and outlet regions attached as shown in Figs. 16 and 18. Unlike the smooth trend observed for the average fluid temperature results, the average wall temperature trend was not smooth and did not correlate well with different aspect ratios and Reynolds numbers. This unusual trend can be attributed to the possible influence of the inlet and outlet regions on the wall temperatures, and the difficulty in obtaining a converged solution for this channel configuration. The addition of the inlet and outlet regions affected the stability of the solution process and many times would diverge to an erroneous solution. Converging to a

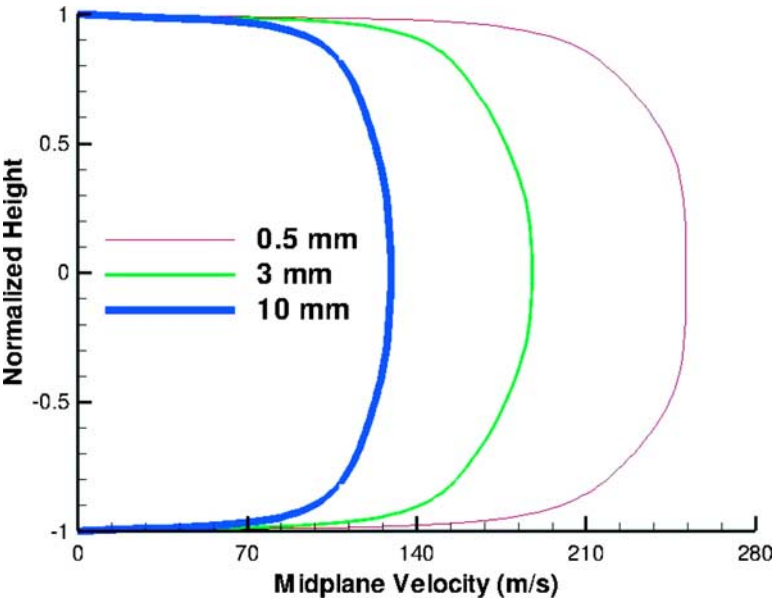

FIG. 13—*Micro-channel length effect on the midplane velocity profile.*

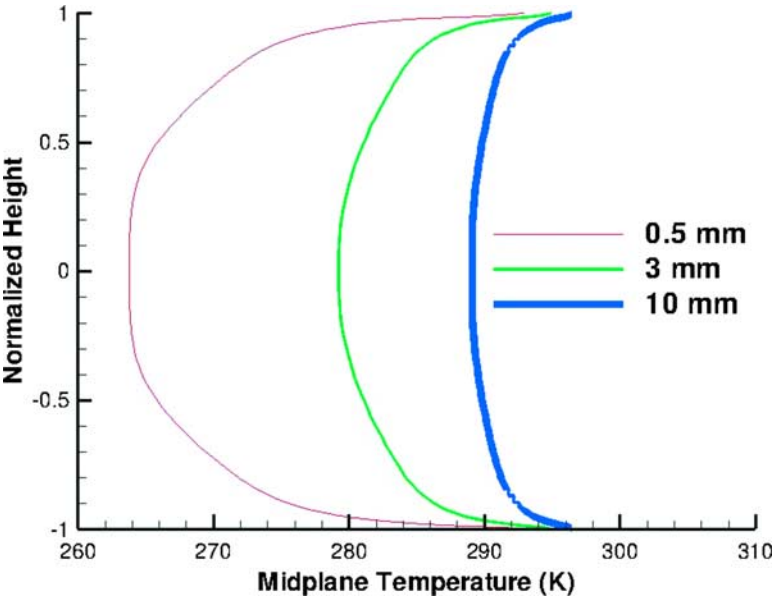

FIG. 14—*Micro-channel length effect on the midplane temperature profile.*

steady-state condition may not have been achieved with this configuration and further work is needed to fully understand the effect of the inlet and outlet attachments on the micro-channel fluid temperature.

Finally, Mach number contours beyond the outlet of a 100 μm height channel are shown in Fig. 19. The Mach number contours suggest that the exiting flow expands supersonically to the ambient atmospheric air. This is an interesting result because the high-speed flow leaving the channel outlet may be of interest to future studies.

Conclusions

A new approach to understanding flow friction ignition that explores whether gas flow could generate the heat required to ignite non-metallic materials in oxygen was described. Oxygen fires attributed to flow friction ignition were presented. A proposed micro-channel gas flow scenario was demonstrated for the

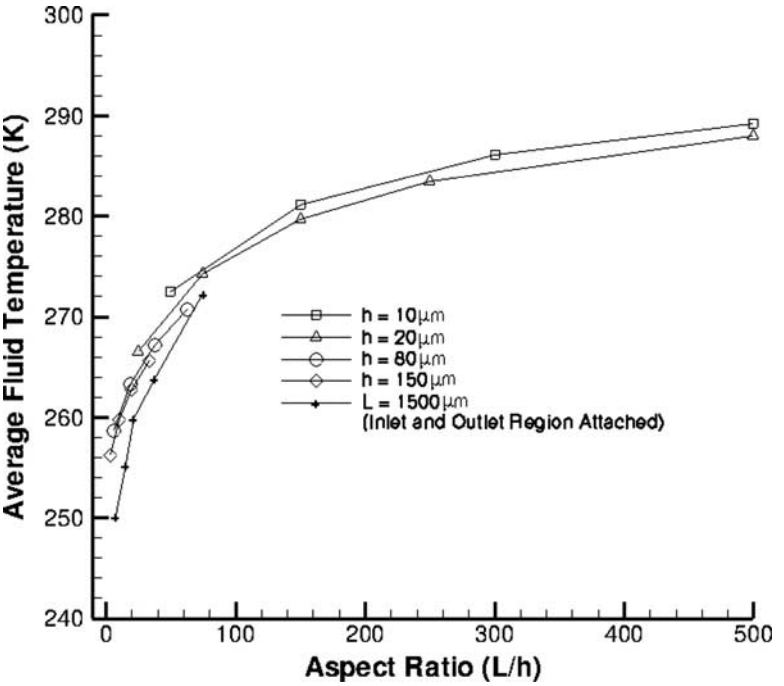

FIG. 15—*Micro-channel aspect ratio and average fluid temperature.*

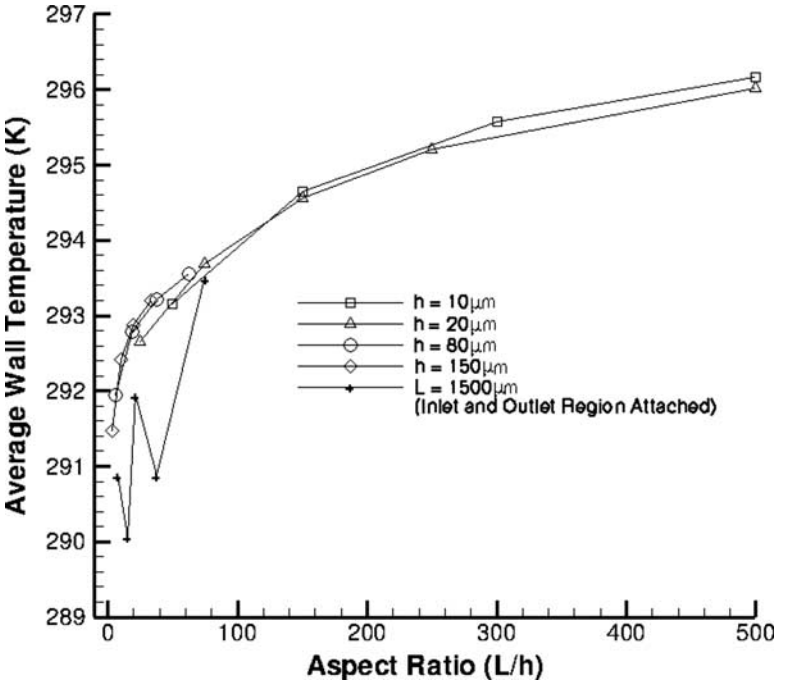

FIG. 16—*Micro-channel aspect ratio and average wall temperature.*

types of non-metallic seals that were identified as fire origin. Micro-channel gas flow was used as the basis to study frictional heating of gas flow through micron-sized cracks in oxygen seals. CFD simulations were shown to be applicable to the study of crack wall temperatures developed by the high-pressure oxygen gas flow and to investigate the heat development within micron-scale channels (i.e., cracks). For the range of micro-channels simulated ($h=10-300$ μm and $L=0.5-10$ mm), viscous effects were most dominant for channels with large aspect ratios and small Reynolds numbers. Average fluid temperatures were approximately 30 K higher for channels with large aspect ratios and small Reynolds numbers than were the average fluid temperatures for channels with small aspect ratios and large Reynolds numbers. Correspondingly, the average wall temperatures were approximately 4 K higher for channels with large aspect ratios and small Reynolds numbers than they were for channels with small aspect ratios and large Reynolds

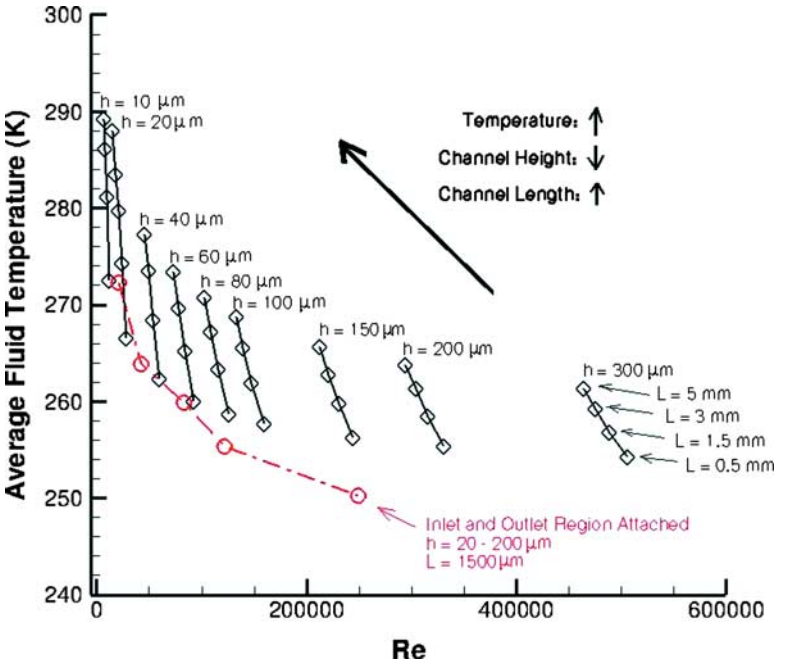

FIG. 17—*Micro-channel Reynolds number and average fluid temperature.*

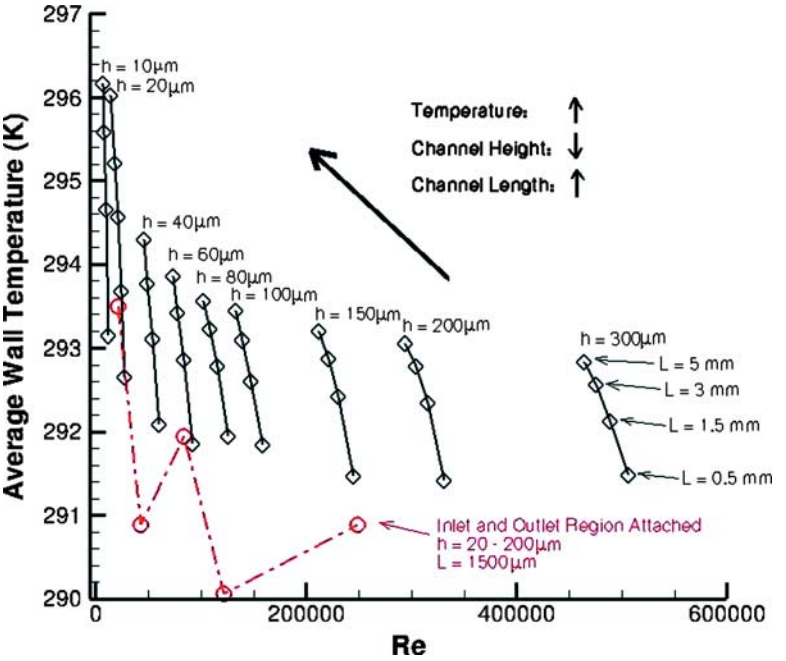

FIG. 18—*Micro-channel Reynolds number and average wall temperature.*

numbers. Although temperatures developed were noticeably different for channels with large aspect ratios, all average fluid and wall temperatures were well below the temperature required to ignite nylon in oxygen (approximately 500 K). Seal cracking probably occurs frequently in nylon seals that are used repeatedly in oxygen systems. Also, if temperatures developed in micro-channel cracks were high, oxygen fires would be expected to occur more frequently. These results suggest that the likelihood of an oxygen fire occurring due to an oxygen leak through a micro-channel crack alone is unlikely and coincides with the rare occurrence of oxygen fires observed in industry. The micro-channel cracks may be one factor that contributes to oxygen fires attributed to flow friction ignition. Other unknown factors or a combination of different factors may join together to explain flow friction ignition in oxygen systems.

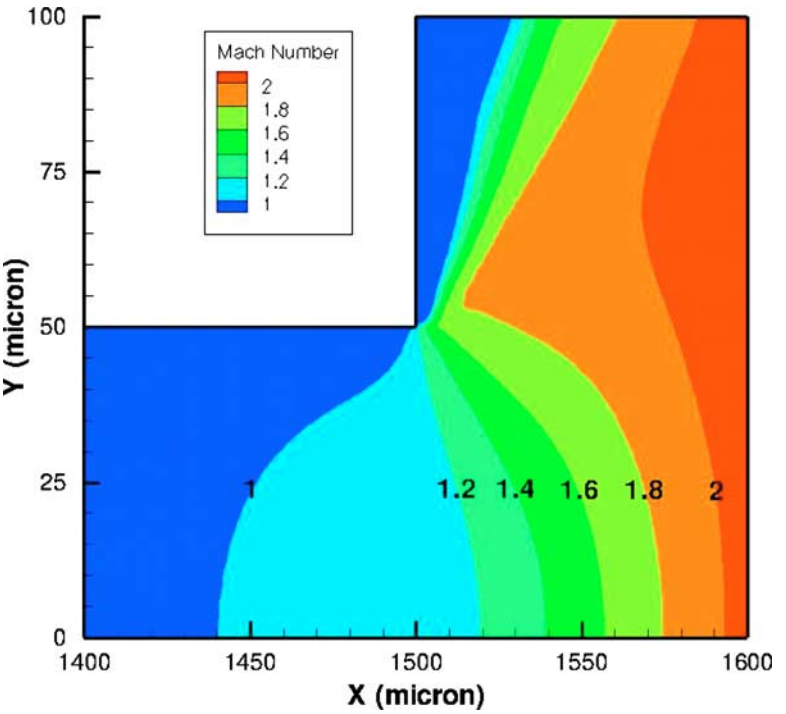

FIG. 19—*Mach number contours beyond the outlet of a 100 μm height channel.*

Future Work

The Fluent® simulation result of supersonic flow at the outlet of the micro-channels may allow for shock wave development and the opportunity for stagnation heating downstream of the channel outlet. The random nature of crack development in nylon seals could provide a configuration that emulates a converging/diverging nozzle (increasing the likelihood of supersonic flow) and that allows nylon obstructions to stagnate the high-speed flow exiting the crack outlet. The heating at these stagnation points may be significant and provokes further investigation as an extension of the high-pressure micro-channel flow friction ignition theory. The identification of micro-channel cracks and the capability for supersonic flow, as simulated by Fluent®, provides a significant contribution and basis for future work.

Finally, interesting information related to localized heating of fatigue crack tips in nylon polymers was discovered in the literature [12]. A hydraulic fatigue test machine induced fatigue cracks in Nylon 6/6 and crack-tip temperatures were recorded with a thermal imaging camera. For one test sample, the localized crack-tip temperature was reported as 55°C and was approximately 30°C higher than the nylon temperature far from the crack-tip region. Future testing may utilize the heat generated at the tip of a propagating nylon crack as another means to explain flow friction ignition of non-metal seals in oxygen.

Acknowlegments

This flow friction ignition research effort was sponsored by Wendell Hull and Associates, Inc. in part to fulfill the requirements of a master's degree at New Mexico State University [13]. Special thanks to Dr. Wendell Hull and the great people of Wendell Hull & Associates, Inc. for their generous support of this project. The writers would like to thank Dr. Chunpei Cai and Dr. Ian Leslie for their contributions to this work.

References

[1] Stong, C. L., *The Scientific American Book of Projects for the Amateur Scientist*, Simon and Schuster Publishing, New York, NY, 1960, pp. 514–520.
[2] Gallus, T. D. and Stoltzfus, J. M., "Flow Friction Fire History and Research," *J. ASTM Int.*, Vol. 3, No. 9, 2006, Paper ID JAI13543.
[3] Ho, C. M. and Tai, T. C., "Micro-Electro-Mechanical Systems (MEMS) and Fluid Flows," *Annu. Rev. Fluid Mech.*, Vol. 30, 1998, pp. 579–612.
[4] Epstein, A. H. and Senturia, S. D., "Macro Power from Micro Machinery," *Science*, Vol. 276, 1997, p. 1211.
[5] Gad-el-Hak, M., "The Fluid Mechanics of Microdevices—The Freeman Scholar Lecture," *ASME J. Fluids Eng.*, Vol. 121, 1999, pp. 5–33.
[6] Kundu, P. K. and Cohen, I. M., *Fluid Mechanics*, 3rd ed., Elsevier Academic Press, New York, NY, 2004, pp. 105–106.
[7] Koo, J. and Kleinstreuer, C., "Liquid Flow in Microchannels: Experimental Observations and Computational Analyses of Microfluidics Effects," *J. Micromech. Microeng.*, Vol. 13, 2003, pp. 568–579.
[8] Beskok, A. and Karniadakis, G. E., "Simulation of Heat and Momentum Transfer in Complex Microgeometries," *J. Thermophys. Heat Transfer*, Vol. 8, 1994, pp. 647–655.
[9] Wu, S., Mai, J., Zohar, Y., Tai, Y. C., and Ho, C. M. "A suspended microchannel with integrated temperature sensors for high-pressure flow studies," *Proceedings of the 11th IEEE Workshop on Micro Electro Mechanical Systems*, 1998, pp. 87–92.
[10] Weast, R.C., *Handbook of Chemistry and Physics*, 54th ed., CRC Press, Cleveland, OH, 1974, p. 195.
[11] Munson, B. R., Young, D. F., and Okiishi, T. H., 2002, *Fundamentals of Fluid Mechanics*, John Wiley and Sons, Inc., New York, NY, p. 4.
[12] Wyzgoski, M. G., Novak, G. E., and Simon, D. L., "Fatigue Fracture of Nylon Polymers: Part 1 Effect of Frequency," *J. Mater. Sci.*, Vol. 25, 1990, pp. 4501–4510.
[13] Hooser, J. D., "A High-Pressure Driven Compressible Gas Flow Study Inside a Two-Dimensional Uniform Microchannel," MS Thesis, New Mexico State University, 2009.